

# Methane bubbles in Lake Kinneret: Quantification and temporal and spatial heterogeneity

Ilia Ostrovsky<sup>1</sup>

Israel Oceanographic and Limnological Research, Yigal Allon Kinneret Limnological Laboratory, P.O. Box 447, Migdal 14950, Israel

## Abstract

The amount of methane bubbles rising from the bottom of Lake Kinneret was quantified by using a dual-beam echo sounder. Both echo-counting (EC) and echo integration (EI) techniques were implemented. Bubbles can confound the identification of fish targets because their acoustic sizes strongly overlap. Analysis of vertical changes in densities in the anoxic hypolimnion (with no fish) indicated that multiple targets were most abundant near the bottom, which caused an essential bias of bubble density estimates by EC. EI was a reliable tool for assessment of bubble density near the bottom. In the upper part of the water column, both techniques provided similar estimates of density of targets (mainly bubbles) because they were measured between dense fish schools during the daytime. The mean acoustic size of rising bubbles decreased in the hypolimnion but increased in the epilimnion, suggesting change in the relative importance of factors controlling gas volume. In summer and fall 2001, the bubbles became predominant echo-reflecting objects in the epilimnion. Temporal and spatial changes in bubble densities were highly heterogeneous, suggesting strong variability in factors affecting the gas ebullition. This variability should be taken into consideration when attempting to quantify the methane ebullition and assessing fish abundance in aquatic systems.

Over the last century, the atmospheric concentration of the greenhouse gas methane has risen ~1% per year (Rowland 1985). The reasons for this trend are not completely understood since the global sources and sinks of methane still need quantification (Conrad and Seiler 1988). Methane is an important product of the anaerobic degradation of organic material in bottom sediments (Kiene 1991). Gas ebullition from the bottom sediments of natural waters could substantially envelop the total methane flux; however, only a few studies have been carried out to assess gas bubble emission from the floor of aquatic ecosystems using different techniques or a combination of methods (e.g., Huttunen et al. 2001; Whiting and Chanton 2001; Leifer and Patro 2002).

Gas traps, video/photo, and acoustic techniques are used to measure gas ebullition. The first two methods are good to quantify gas emission in confined areas. Acoustic methods might be helpful to evaluate spatial variability of bubbles, which are strong scatterers of acoustic energy, in deep enough aquatic systems (Vagle and Farmer 1991; Jackson et al. 1998; Hornefius et al. 1999; Quigley et al. 1999). Acoustic remote-sensing methods offer the advantage of being able to quickly scan large volumes of the water column synoptically, but they typically lack the ability to resolve and taxonomically classify individual targets. Gas bubbles rising from the bottom can contaminate the assessment of fish densities with echo sounders (Rudstam and Johnson 1992).

In this study, I used a dual-beam echo sounder to quantify bubble densities in the water column of a stratified lake. I compared results of the echo-counting (EC) and echo integration (EI) techniques in order to evaluate the appropriate method for assessment of bubble density in water. I further examined the seasonal and spatial variability in bubble density in Lake Kinneret.

## Materials and methods

*Study site*—Lake Kinneret is a warm subtropical lake with a maximum depth of 36.5–43 m (depending on lake level). The water level usually fluctuates within a 4-m interval (between 209 and 213 m below sea level). In 2001, the lake level dropped about 6 m below its upper limit because of a few consecutive dry seasons and excessive water supply to the Israeli National Water Carrier. The lake is thermally stratified from March/April until December. During that time, there is an increase of near-bottom dissolved methane concentrations and amount of gas (>90% methane) captured by gas traps located in the hypolimnion (Eckert unpubl. data). Between June and December, the hypolimnion is enriched by hydrogen sulfide, thereby limiting the fish distribution to regions shallower than the hypolimnion (Walline et al. 1992). Other echo-reflecting objects (i.e., gas bubbles) have not previously been quantified in the lake.

*Data acquisition*—Spatial and temporal changes in acoustic target abundance were examined based on data collected from June to December 2001, when the lake was strongly stratified and gas bubbles were the only targets in the anoxic hypolimnion. Data were sampled along the following transects: one transect was positioned in the central, deepest part of the lake (bottom depth: 35–38 m) and three transects were located between the eastern shore and the lake interior. For details of transect locations see Ostrovsky and Walline (2001). A GPS unit was used to assure coverage of the same

<sup>1</sup> Corresponding author (Ostrovsky@ocean.org.il).

## Acknowledgments

I thank Y. Kipnis for his assistance with data processing and J. Didenko, J. Easton, S. Kaganovsky, and M. Hatab, from the Kinneret Limnological Laboratory for faithful technical assistance with the fieldwork. I also thank G. Gal for the fruitful discussions and for his valuable comments. I am grateful for the constructive criticism of two anonymous reviewers whose useful suggestions greatly improved the manuscript. This study was supported by grants from the Israel Water Commissioner and the Israel Science Foundation (211/02).

transects. The surveys were carried out using a Biosonics dual-beam Scientific Echosounder DE5000 (6.5° half-power narrow beam width) operating at 120 kHz, a pulse width of 0.2 ms, and a ping rate of 5 pings  $s^{-1}$ . The acoustic system was regularly calibrated with a standard target (Foote et al. 1987). The calibrations showed no change from the manufacturer's calibration. Lower threshold for data collection was set to  $-75$  dB. A minimum bottom-scattering strength of  $-35$  dB was chosen for bottom detection. Data were collected between 1 m from the transducer and 0.5 m above the bottom (maximum distance from the transducer was 38 m). Acoustic measurements were accompanied by CTD profiling in the middle of each transect to determine thermocline position.

To resolve the acoustic backscatter from individual fish and to allow the use of EC techniques, most of our surveys were carried out at night, when single targets predominated (80–90% of total number of targets), as fish were loosely aggregated.

A special day survey along the deepest central transect was carried out on 17 October 2001, when most of the fish were in dense schools and no fish tracks could be detected on echograms of the interschool water volume. Several transect sections located between fish schools were selected and analyzed in order to minimize the influence of fish on size-frequency distributions and target densities in the upper stratum. All data from the chosen sections were treated together. EC methods were implemented to study vertical changes in size-frequency distributions and target density in the water column.

Data were processed with the Biosonics Visual Analyzer software (version 4.02) to a vertical resolution of 1 m. This program automatically compensates the received echo signals (voltage) depending on the range ( $R$ , m) of the target/layer by time-varied gain (TVG). A  $40 \log_{10}(R)$  TVG is applied for echo counting and the measurement of target size, whereas a  $20 \log_{10}(R)$  TVG is applied when echo integrating. The dual-beam echo sounder allows identification of the position of a single target within the acoustic beam by joint processing of the narrow- and wide-beam data, thus estimating its acoustic size in situ. The acoustic size of an individual target is given as the backscattering cross-section,  $\sigma_{bs}$ , or as its logarithmic equivalent, the target strength (TS),  $TS = 10 \log_{10}(\sigma_{bs})$ . To obtain accurate assessments of TS-frequency distribution, a single target filter was applied. Pulses narrower than the transmission pulse, with a width factor  $>1.2$  and correlation factor  $<0.96$  (calculated by the Biosonics Visual Analyzer software) were excluded. Targets assessed at  $>3$  dB off the acoustic axis were also rejected. The mean acoustic size of targets was calculated based on measured  $\sigma_{bs}$ , then the mean  $\sigma_{bs}$  was converted to TS. The lower and upper 95% confidence limits of the mean  $\sigma_{bs}$  were also calculated and expressed as TS limits. Target abundance is reported in terms of total number of targets within the  $-75$  to  $-35$  dB range and are binned into 1-dB TS bins.

Acoustic data collected in the anoxic strata were echo integrated to estimate the volumetric density of bubbles during night and day surveys. EI procedure was also applied to the data collected between fish schools during the day survey (see above) to quantify vertical changes in target densities

for the entire water column. For each transect, the volume backscattering coefficient,  $s_v$ , was calculated in bins of 3 m depth and 200 m horizontal length, defining  $\sim 12$ – $15$  sampling units at each depth layer. The volumetric density of targets per cubic meter ( $N$ ) in each bin was estimated using the mean  $\sigma_{bs}$  to scale the  $s_v$  (i.e.  $N = s_v/\sigma_{bs}$ ). The average volumetric densities ( $\pm 95\%$  confidence limits) were calculated for a 3-m layer, when vertical variations were considered, and for the entire hypolimnetic part of the water column when seasonal or lateral changes were examined. For more details about hydroacoustic methods see, for example, Urick (1975), Clay and Medwin (1977), and MacLennan and Simmonds (1992).

## Results and discussion

*Visual inspection of echograms*—Fish and gas bubbles are the two main echo-reflecting objects in Lake Kinneret. During night surveys, when fish were loosely dispersed, it was not always possible to differentiate between these kinds of targets from inspection of acoustic echograms, which were recorded at the fast survey speeds, in shallow strata, or both. In contrast, bubbles and fish were easily distinguished on deep sections of the echograms if the acoustic surveys were carried out at a low speed and the same objects were detected over the course of many consecutive pings. In such cases, single fish were characterized by near-horizontal traces, whereas bubbles had inclined ones. The slower the boat speed, the clearer difference between bubbles and fish traces (Fig. 1A, 1B). Visual analyses of the echograms recorded on the drifting stations (the boat speed was usually up to 0.5 knots) allowed us to see the ascent of bubbles from the bottom. In some cases, traces split on their way up (Fig. 1C). This could be a result of breaking up of large bubbles into small ones or the effect of spatial divergence of a few close-positioned bubbles that had been released from the bottom nearly simultaneously but could not be distinguished by the acoustic system (multiple targets). Visual analyses of many echograms from the day survey performed at speeds of  $\sim 4$  knots at the central lake locations (where concentrations of fish are usually lower than at the lake periphery; Ostrovsky et al. 1996) revealed that the majority of targets seen in the interschool volume were bubbles (Fig. 1D). Bubbles rising from the bottom were frequently seen as numerous target chains or columns. Continuous streams of bubbles and intermittent bursts of four or five bubbles commonly have been observed in many natural seeps (e.g., Hovland and Judd 1988).

*Vertical changes in bubble characteristics*—The results of day acoustic sampling between fish schools are presented in Fig. 2. TS-frequency distributions obtained for the anoxic hypolimnion (where only bubble targets were present) and oxic epilimnion were nearly identical (Fig. 2A). It suggests that during the day, most targets collected between the schools could be attributed to gas bubbles. In contrast, the distribution of acoustic targets in the epilimnion during the preceding night sampling, when fish were loosely dispersed, was different from that of bubbles.

The geometric size of a bubble can be roughly inferred

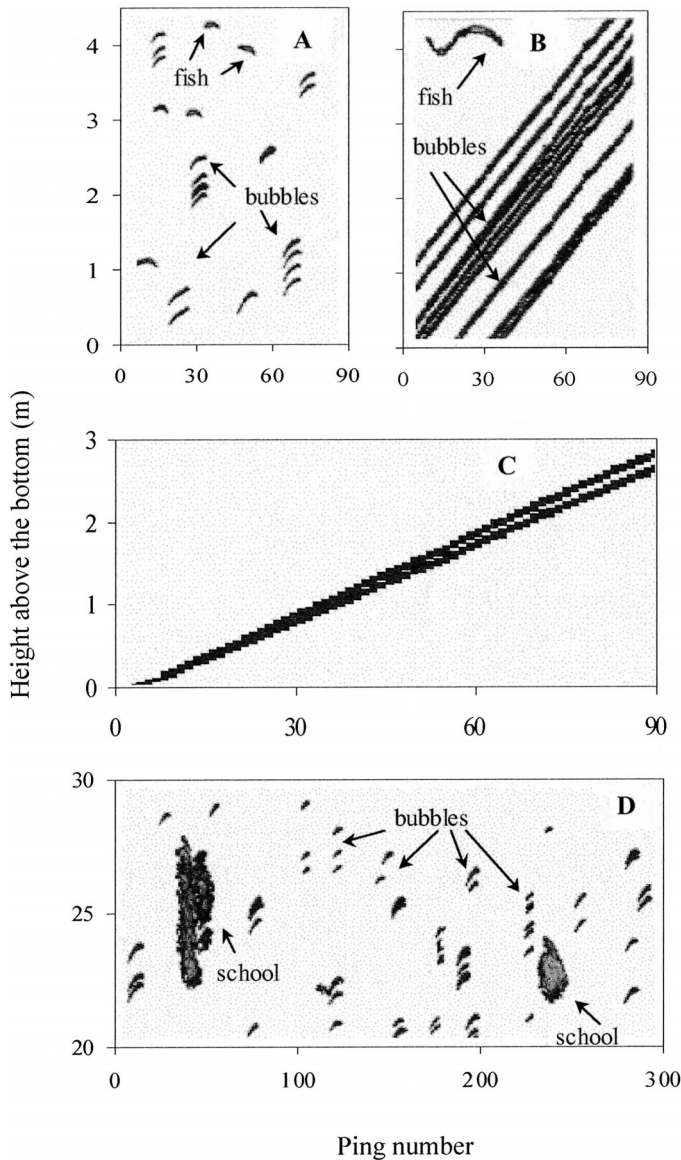


Fig. 1. Echograms show bubble and fish traces during acoustic surveys. (A) Bubble and fish tracks at a survey speed of ~4 knots (night survey). (B) Bubble and fish tracks at a survey speed of <0.2 knots (night survey). (C) Bubble traces split on their way up from the bottom (survey speed <0.2 knots). (D) Bubbles between the fish schools (day survey, speed ~4 knots).

from its acoustic size, assuming that bubble has no resonance close to the echo sounder frequency (Clay and Medwin 1977). To comply with this assumption and given the frequency of 120 kHz and depth range down to 38 m, the resonant bubble radius is  $\leq 0.06$  mm (see the formulae in Urick 1975). Observations on bubble ascent with time on drifting stations allowed us to calculate the mean rising velocity of bubbles as  $0.22 \pm 0.1$  cm s<sup>-1</sup>. This velocity could be reached by clean bubbles of ~0.6 mm radius or dirty bubbles with a radius of up to a few millimeters (Leifer and Patro 2002). Such bubbles are apparently too large to resonate. For a nonresonant bubble, whose radius,  $r$ , is notably less than the wavelength (i.e.,  $r \ll 12$  mm at 120 kHz), the

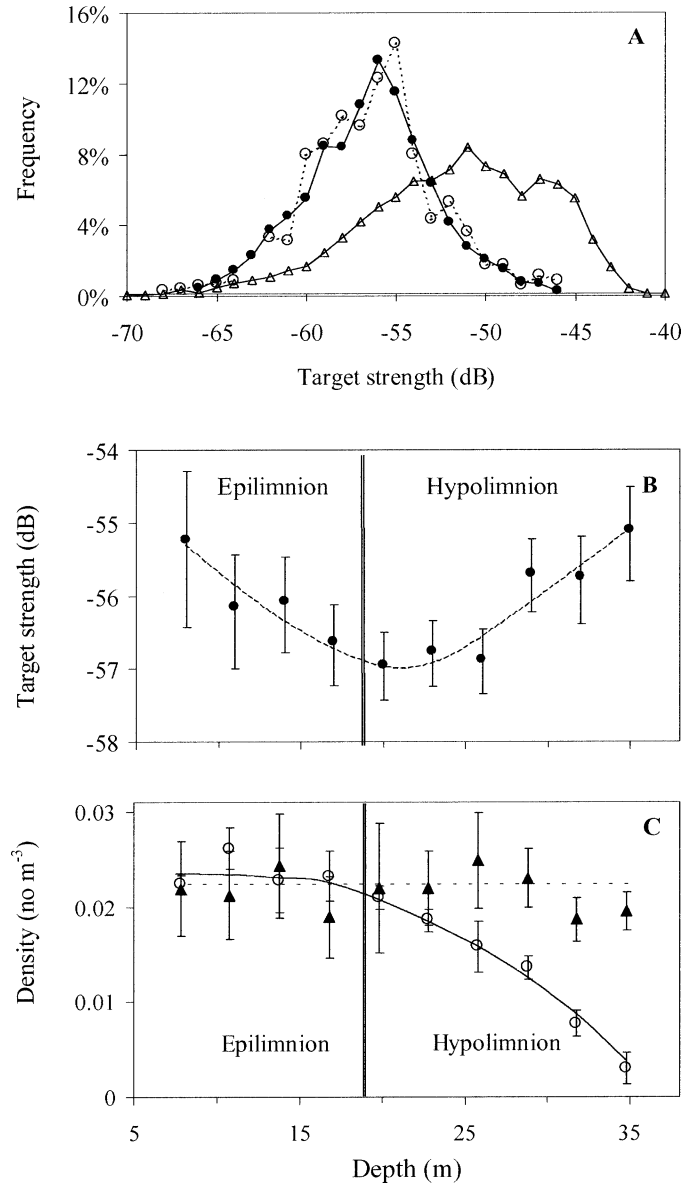


Fig. 2. TS measurements and target densities from daytime (17 October 2001) acoustic sampling between fish schools. Data represent acoustic sizes of gas bubbles in the deepest part of Lake Kinneret. (A) TS-frequency distributions in the anoxic hypolimnion (filled circles) and in the oxic epilimnion (open circles). For comparison, distribution of targets in the epilimnion during nighttime (fish were loosely dispersed) on 16 October 2001 is shown by open triangles. Results of dual-beam analysis. Total number of targets in the epilimnion and hypolimnion on 17 October was 700 and 3,197, respectively, and in the epilimnion on 16 October was 6,921. (B) Vertical changes in average TSs of bubble targets in the water column (vertical resolution of 5 m). Results of dual-beam analysis. Vertical double line shows thermocline position. Thin bars are 95% confidence intervals. (C) Echo-counting (open circles) and echo integration (filled triangles) vertical profiles of bubble densities in the water column. Horizontal line indicates the EI average density in the entire water column. Vertical double line shows thermocline position.

ratio of the scattering cross section,  $\sigma_s$ , to the geometric cross section,  $\pi r^2$ , approaches 4 (Urlick 1975). Because bubble scatter is omnidirectional,  $\sigma_s = 4\pi\sigma_{bs}$ . Then,  $r = (\sigma_{bs})^{1/2}$ . This relationship allows approximation of bubble radius from  $\sigma_{bs}$  (or TS). Translation of the TS-frequency distribution (Fig. 2A) to the radius-frequency distribution suggests that 95% of bubble radii ranged from 0.6 to 3.3 mm. Bubbles of such sizes are commonly reported for natural hydrocarbon seeps (e.g., Leifer et al. 2000a).

Within the hypolimnion, the average acoustic size of bubbles slightly decreased from the near-bottom stratum to the upper hypolimnion (Fig. 2B) and then gradually increased from the upper hypolimnion toward the lake surface. Decreases in TS on bubble ascent within the hypolimnion were also registered on other transects and on different sampling dates. The alteration in acoustic size of the rising bubbles can be caused by a combined effect of volume expansion when hydrostatic pressure drops and asymmetric exchange of gases with surrounding water. Numerical simulations of rising bubbles showed that their fate strongly depends on depth of gas release, initial size of emitted bubble, vertical speed of ascent, aqueous concentration of methane and atmospheric gases, and temperature (Leifer and Patro 2002). For instance, the model indicated that volume of a small bubble (e.g.,  $r = 0.25$  mm) notably decreases as it rises, whereas the volume of a large bubble (e.g.,  $r = 2.5$  mm) increases. In our case, the reduction in the mean bubble sizes in the anoxic hypolimnion (Fig. 2B) could be associated with the predominance of the methane outflow.

In the upper aerated strata where the dissolved air inflow could partially compensate for the methane outflow, the increase in the mean bubble size could be associated with the reduction of hydrostatic pressure. The expected change in bubble TS from pressure drop can be computed using some assumptions. Given a proportionality of the acoustic size with the geometric cross section and assuming isometric changes in bubble dimensions, one can calculate that, in accordance with Boyle's law, the increase in TS between 20- and 8-m layers should be 1.5 dB. The good correspondence of the observed (Fig. 2B) and calculated changes in TS suggests that hydrostatic pressure was apparently the major factor affecting the mean TS value in the upper part of the water column. The occurrence of a small number of fish between schools could also enlarge the mean TS value in the epilimnion; however, the effect of residual fish was negligible because the TS-frequency distributions in the epilimnion and hypolimnion completely differ from that of the mixture of fish and bubbles (Fig. 2A).

To quantify the changes in densities of acoustically visible targets in the water column, the EC techniques were applied to the data sampled between fish schools during the daytime. The results clearly indicate that bubble density counted near the bottom dramatically increased (by an order of magnitude) toward the upper part of the hypolimnion. This result agrees with our visual inspection of the echograms indicating that some traces "separated" into several small ones upon ascent within the hypolimnion (*see above*). As soon as bubbles penetrated into the highly turbulent epilimnion, there was little change in bubble density (Fig. 2C). Breakup of bubbles because of volume expansion cannot explain the

observed vertical changes in target density because gas volume increases to a greater extent in shallower than in deeper strata. Besides, underwater observations made on hydrocarbon seeps did not reveal a breakup of rising bubbles (Leifer et al. 2000b). Dispersion of closely positioned ("packed") bubbles by turbulent motions in the water column or because of variability in ascent velocity could increase the density of the acoustically visible targets from the bottom to the thermocline. As soon as the majority of the packed bubbles had diverged sufficiently to be counted as individuals, no further changes in target density should be detected. The latter justified the vertical homogeneity of bubble density in the upper part of the water column. The increased proportion of multiple targets in deeper strata also could be related to a higher probability of including multiple echos as single targets because the critical target density, above which EC gives biased results, decreases as the square of the distance from the transducer (MacLennan and Simmonds 1992). The observed sharp vertical changes in bubble abundance with distance from the bottom indicates that the assumption about similarity of bubble densities in the hypolimnion and epilimnion, which frequently has been used for calculation of fish abundance using hydroacoustic techniques (e.g., Jurvelius and Sammalkorpi 1995), cannot be implemented without testing.

To compare vertical profiles of bubble densities obtained from EC and EI, the volume backscattering was scaled to volumetric densities (bubbles  $m^{-3}$ ) using the mean stratum-specific TSs calculated from dual-beam processing (Fig. 2B). Data collected between schools of fish in the upper oxic strata could be potentially contaminated by the presence of individual fish. This would modify  $s_v$  and  $\sigma_{bs}$  to a greater extent than bubble density. However, analysis of TS-frequency distribution (*see above*) indicated that the effect of fish on the mean TS was unimportant. In contrast to the changes observed from the EC, the volume backscattering and calculated densities of bubbles were nearly invariable over the entire water column (Fig. 2C). The latter confirms our suggestions that the difference in percentages of multiple targets could affect the bubble density obtained using the EC methods for the hypolimnion. The average target density in the whole-water column obtained by the EI ( $0.022 \pm 0.004$  bubbles  $m^{-3}$ ) was close to bubble abundance in the epilimnion evaluated by the EC procedure ( $0.024 \pm 0.001$  bubbles  $m^{-3}$ ). The similarity of the abundance estimates and constancy of the bubble densities within the epilimnetic and hypolimnetic parts of the water column obtained by different techniques suggests that (1) most bubbles released from the bottom do not physically split into smaller ones, as might be expected from target counting in the hypolimnion; (2) EI can be used for good assessment of bubble density in the entire water column based on data collected in the anoxic hypolimnion.

*Seasonal dynamics and spatial variability*—To evaluate the temporal and spatial changes in bubble abundance, the data recorded in the anoxic hypolimnion during the regular night surveys were echo integrated. In each case, the mean backscattering cross-section was determined for the hypolimnion and applied as a scaling factor to the volume backscatter. The mean acoustic size of bubbles varied with time

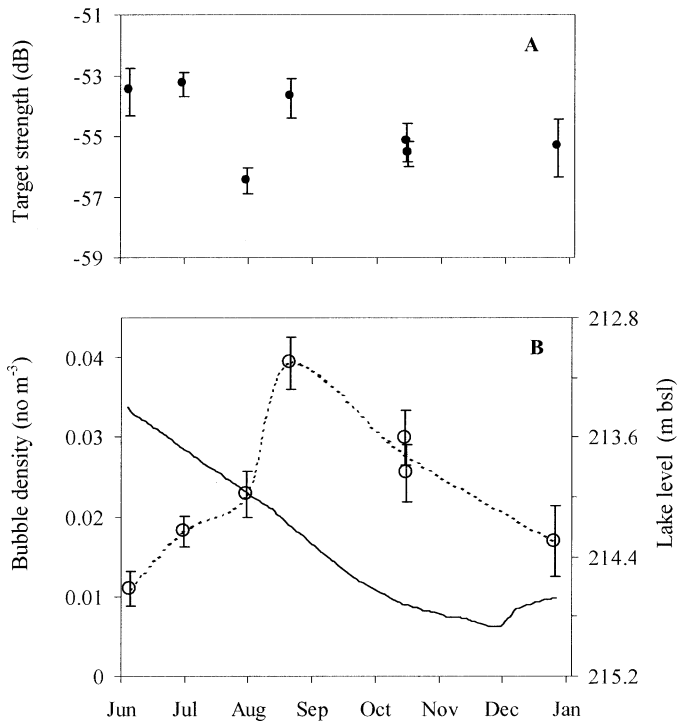


Fig. 3. Seasonal changes in the mean acoustic size and density of bubbles in the central part of Lake Kinneret. (A) The mean acoustic sizes of bubbles in the hypolimnion. (B) The mean volumetric densities of bubbles (open circles) and water level in the lake (solid line). Bubble densities were estimated for the anoxic hypolimnion based on the EI method. The mean acoustic sizes (panel A) were used as scaling factors for EI. Vertical lines represent 95% confidence intervals.

(Fig. 3A). The changes in size were statistically significant ( $P < 0.01$ ) for some distant sampling dates, whereas for the adjacent sampling dates (16 and 17 October 2001), the mean sizes were nearly identical. A slight declining trend in the mean size of bubbles was noticed ( $R = -0.57$ ,  $P < 0.05$ ) for the entire sampling period; however, the decrease in the equivalent bubble radius was small (from 2.1 mm in June to 1.7 mm in October–December 2001). The mean target sizes at different sampling locations altered coherently (data not shown). Possibly, the sizes of emitted bubbles could be associated with growth and subsequent reduction of gas pressure in sedimentary reservoirs.

The data collected at the central location showed clear seasonal changes in bubble density (Fig. 3B). In accordance with the temporal variations of bubble densities (reflecting the changes in intensity of gas ebullition from the bottom), the contribution of bubbles to the total amount of acoustic targets (fish and bubbles) in the epilimnion also changed (Fig. 4). The proportion of bubble targets reached up to 70% of the total amount of all targets in the epilimnion in August 2001. Taking into account that the TS of small fish (young-of-the-year) and bubbles strongly overlap, methane ebullition can cause a strong bias in assessment of fish density and TS-frequency distribution.

The processes affecting gas emission from the lake/sea bottom are not clearly understood yet. Alterations of the

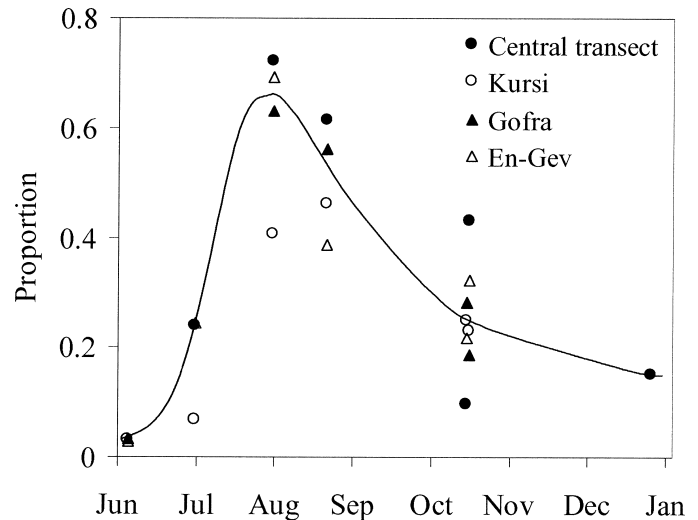


Fig. 4. Contribution of bubbles to the total amount of acoustic targets (fish and bubbles) in the epilimnion at the central transect, Kursi, Gofra, and En-Gev. Target densities were computed based on the EI method (see the text).

pressure at the bottom related with fluctuations of water level, atmospheric pressure (Mattson and Likens 1987; Dove et al. 1999), and tidal effect (Martens and Klump 1980) can determine changes in gas ebullition. Zimov et al. (1997) indicated that in thermokarst lakes, methane fluxes were highest when deep sediments had their annual thermal maximum. In Lake Kinneret, large seasonal fluctuations of water level could play a key role in temporal changes in emission of gaseous methane, since variations of bottom temperature and air pressure could affect the volume of benthic gas reservoirs to a much lesser extent. In fact, the highest amount of bubbles in the water was observed between July and November, coinciding with a sharp decline in lake level and a respective decrease in hydrostatic pressure at the bottom. Such a decrease might cause expansion of sedimentary reservoirs and gas emission to the overlying water. Dramatic increases in bubble concentrations were observed from June until the end of August. The June enlargement occurred when the water level dropped below the lowest level recorded in the preceding year (213.7 m below sea level). The peak of August was associated with the highest rate of water level descent ( $12.5 \text{ cm d}^{-1}$ ) during the second half of August. The decrease in the rate of water level drop since mid-September ( $10 \text{ cm d}^{-1}$ ) to mid-October ( $3.5 \text{ cm d}^{-1}$ ) resulted in a decrease in the amount of bubbles in the water. Stabilization of the water level in November–December associated with the beginning of the winter season reduced the intensity of bubble emission and bubble density in the water.

Acoustic sampling carried out along three sloped offshore transects (directed from the shoreline to the lake interior) showed lateral alterations in bubble densities. Examples given in Fig. 5 illustrate different patterns of bubble density changes along various transects. In one case (Fig. 5A), the bubble density increased from the shallower toward the deepest locations; in a second case (Fig. 5B), the density displayed a reverse trend; and in the third case (Fig. 5C), there was a distinct maximum in bubble density close to the

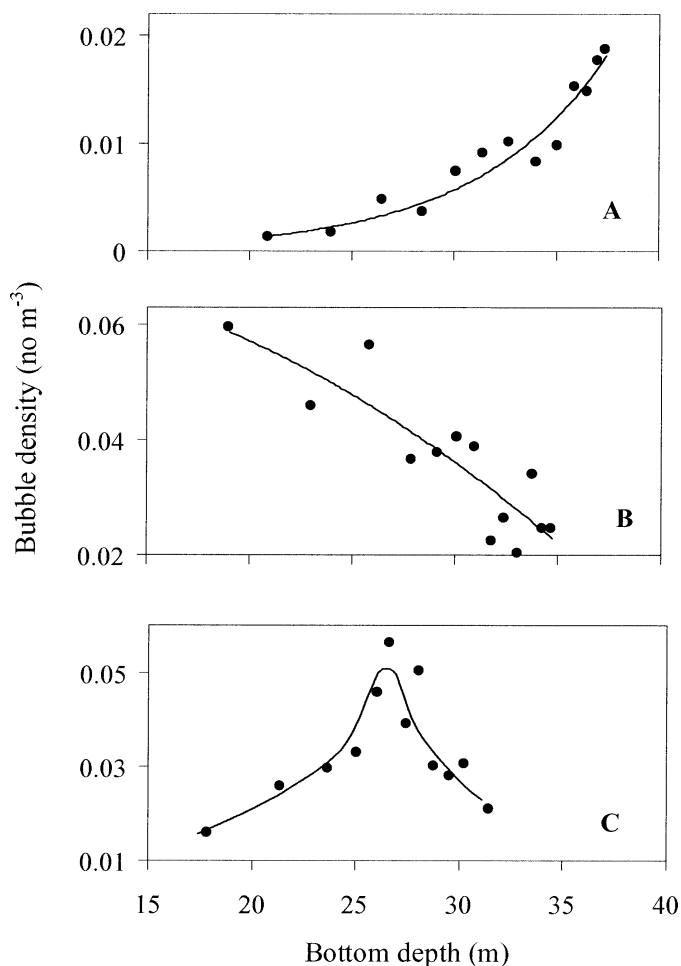


Fig. 5. Typical examples of lateral changes in bubble densities along three sloped transects. At each transect, bottom depth increases with distance from the shoreline. Volumetric densities of bubbles were estimated based on the EI method from the data sampled in the anoxic hypolimnion. (A) Kursi transect on 2 July 2001. The mean TS applied to EI was  $-54.9$  dB. (B) Gofra transect on 22 August 2001. The mean TS applied to EI was  $-55.1$  dB. (C) En-Gev transect on 1 August 2001. The mean TS applied to EI was  $-57.8$  dB.

center of the transect. The observed lateral variations in gas emission patterns could be associated with two or more factors. A decline in the water level could swell the sedimentary gas reservoirs such that, in shallower locations, their volumes expand to a larger extent than those in deeper locations. The latter is determined by a higher relative change in pressure at the bottom in the shallower locations. Such asymmetrical changes in volume of gas reservoirs should induce differences in gas ebullition when water level drops. On the other hand, an increase in bubbling intensity with depth might be determined by a higher rate of methane production in the deeper locations because of a focusing of organic-rich settling particles (Ostrovsky and Yacobi 1999) and the resulting decomposition of their organic components within the bottom sediments. In fact, sedimentary focusing can result in a higher rate of methane production and storage under the bottom in the deeper part of the lake. The emitted

methane could have been produced during various time spans and trapped within the sediment. For instance, Zimov et al. (1997) reported that half of the emitted methane in Siberian lakes derived from Pleistocene-aged carbon. Other factors, such as sediment porosity, cohesiveness, granulometric composition, temperature differences, underwater seeps, and near-bottom currents might also affect the gas ebullition intensity. In addition, one can consider a possible effect of microseismic activity around the lake (Ben-Avraham et al. 1981), which might facilitate unequal gas release from the sediment. The role of the above-mentioned factors and processes in emission of sedimentary gases is not clearly understood yet and should be a subject of future investigations.

The drastic temporal and spatial changes in concentrations of gas bubbles in water should be taken into consideration for quantification of methane emissions and for accurate assessment of fish abundance in lakes.

### References

- BEN-AVRAHAM, Z., A. GINZBURG, AND Z. YUVAL. 1981. Seismic reflection and refraction investigations of Lake Kinneret—central Jordan Valley. *Tectonophysics* **80**: 165–181.
- CLAY, C. S., AND H. MEDWIN. 1977. *Acoustical oceanography: Principles and applications*. Wiley-Interscience.
- CONRAD, R., AND W. SEILER. 1988. Methane and hydrogen in sea water (Atlantic ocean). *Deep-Sea Res.* **12**: 1903–1917.
- DOVE, A., N. ROULET, P. CRILL, J. CHANTON, AND R. BOURBONNIERE. 1999. Methane dynamics of a northern boreal beaver pond. *Ecoscience* **6**: 577–586.
- FOOTE, K. G., H. P. KNUDSEN, G. VESTNES, D. N. MACLENNON, AND E. J. SIMMONDS. 1987. Calibration of acoustic instruments for fish density estimation: A practical guide. International Council for Exploration of the Sea Cooperative Research Rep. 144.
- HORNAFIUS, J. S., D. C. QUIGLEY, AND B. P. LUYENDYK. 1999. The world's most spectacular marine hydrocarbon seeps (Coal Oil Point, Santa Barbara Channel, California): Quantification of emissions. *J. Geophys. Res.* **104**: 703–720.
- HOVLAND, M., AND A. G. JUDD. 1988. Seabed pockmarks and seepages. Graham and Trotman.
- HUTTUNEN, J. T., T. HAMMER, J. ALM, J. SILVOLA, AND P. J. MARTIKAINEN. 2001. Greenhouse gases in non-oxygenated and artificially oxygenated eutrophic lakes during winter stratification. *J. Environ. Qual.* **30**: 387–394.
- JACKSON, D. R., K. L. WILLIAMS, T. F. WEVER, C. T. FRIEDRICH, AND L. D. WRIGHT. 1998. Sonar evidence for methane ebullition in Eckernförde Bay. *Cont. Shelf Res.* **18**: 1893–1915.
- JURVELIUS, J., AND I. SAMMALKORPI. 1995. Hydroacoustic monitoring of the distribution, density and mass-removal of pelagic fish in a eutrophic lake. *Hydrobiol.* **316**: 33–41.
- KIENE, R. P. 1991. Production and consumption of methane in aquatic systems, p. 111–146. *In* J. E. Rogers and W. B. Whitman [eds.], *Microbial production and consumption of greenhouse gases: Methane, nitrogen oxides and halomethanes*. American Society for Microbiology.
- LEIFER, I., AND R. K. PATRO. 2002. The bubble mechanism for methane transport from the shallow sea bed to the surface: A review and sensitivity study. *Cont. Shelf Res.* **22**: 2409–2428.
- , J. F. CLARK, AND R. F. CHEN. 2000a. Modifications of the local environment by natural marine hydrocarbon seeps. *Geophys. Res. Lett.* **27**: 3711–3714.
- , R. K. PATRO, AND P. BOWYER. 2000b. A study on the

- temperature variation of rise velocity for large clean bubbles. *J. Atmos. Ocean. Technol.* **17**: 1392–1402.
- MACLENNAN, D. N., AND E. J. SIMMONDS. 1992. *Fisheries acoustics*. Chapman & Hall.
- MARTENS, C. S., AND J. V. KLUMP. 1980. Biogeochemical cycling in an organic-rich coastal marine basin. I. Methane–sediment exchange processes. *Geochim. Cosmochim. Acta* **44**: 471–490.
- MATTSON, M. D., AND G. E. LIKENS. 1987. The effect of barometric pressure on methane ebullition rates. *Eos* **68**: 1691.
- OSTROVSKY, I., AND P. WALLINE. 2001. Multiannual changes in the pelagic fish *Acanthobrama terraesanctae* in Lake Kinneret (Israel) in relation to food sources. *Verh. Int. Verein. Limnol.* **27**: 2097–2094.
- , AND Y. Z. YACOBI. 1999. Organic matter and pigments in surface sediments: Possible mechanisms of their horizontal distributions in a stratified lake. *Can. J. Fish. Aquat. Sci.* **56**: 1001–1010.
- , ———, P. WALLINE, AND Y. KALIKHMAN. 1996. Seiche-induced water mixing: Its impact on lake productivity. *Limnol. Oceanogr.* **41**: 323–332.
- QUIGLEY, D. C., J. S. HORNAFIUS, B. P. LUYENDYK, R. D. FRANCIS, J. CLARK, AND L. WASHBURN. 1999. Decrease in natural marine hydrocarbon seepage near Coal Oil Point, California, associated with offshore oil production. *Geology* **27**: 1047–1050.
- ROWLAND, F. S. 1985. Methane and chlorocarbons in the earth's atmosphere. *Origins Life* **15**: 279–297.
- RUDSTAM, L. G., AND B. M. JOHNSON. 1992. Development, evaluation and transfer of new technology, p. 507–524. *In* J. F. Kitchell [ed.], *Food web management: A case study of Lake Mendota*. Springer-Verlag.
- URICK, J. U. 1975. *Principles of underwater sound*. McGraw-Hill.
- VAGLE, S., AND D. M. FARMER. 1991. The measurements of bubble-size distribution by acoustic backscatter. *J. Atmos. Ocean. Technol.* **9**: 630–644.
- WALLINE, P., S. PISANTY, AND T. LINDEM. 1992. Acoustic assessment of number of pelagic fish in Lake Kinneret. *Hydrobiologia* **231**: 153–163.
- WHITING, G. J., AND J. P. CHANTON. 2001. Greenhouse carbon balance of wetlands: Methane emission versus carbon sequestration. *Tellus* **53**: 521–528.
- ZIMOV, S. A., AND OTHERS. 1997. North Siberian lakes: A methane source fueled by Pleistocene carbon. *Science* **277**: 800–802.

Received: 8 July 2002

Accepted: 23 January 2003

Amended: 5 February 2003